Heat and Mass Transfer During the Dissociation of Hydrates in Porous Media

M. S. Selim
E. D. Sloan
Chemical Engineering Department
Colorado School of Mines
Golden, CO 80401

Gas hydrates are crystalline ice-like solids that form when water and sufficient quantities of certain gases, relatively small in molecular size, are combined under the right conditions of temperature and pressure. Under these conditions, the amount of gas stored in a given volume of hydrate is 170 times higher than when the gas is at standard conditions. This fact contributes to its potential as an economically recoverable energy source.

Substantial amounts of hydrates have been found in the earth's sediment beneath the permafrost, in Arctic basins, and in ocean bottom sediments along the continental margins of the United States. Due to this potential resource, the problems associated with the production of natural gas from these hydrate zones have become of greater interest to the hydrocarbon industry. Preliminary simulation studies for the production of gas from hydrate reservoirs using thermal injection, depressurization, and *in-situ* combustion have been done by McGuire (1981), Holder et al. (1982), and others. However, one area which is important but has received little attention is the rates of heat and mass transfer during hydrate dissociation. Kamath et al. (1984) viewed hydrate dissociation as a nucleate boiling phenomenon. Selim and Sloan (1985) viewed heat transfer during hydrate dissociation as a moving-boundary ablation process and showed that their model fits hydrate dissociation data to within 10% (Ullerich et al., 1987). Results of these studies are only useful in modeling pure hydrate dissociation processes.

For gas hydrates in the earth's sediment, the rates of heat and mass transfer are strongly influenced by the presence of the surrounding sediment. In the present work, a physical model that describes hydrate dissociation under thermal stimulation in porous media, is presented. The model views the dissociation as a process whereby gas and water are produced at a moving boundary. The latter separates the dissociated zone, which contains gas and water, from the undissociated zone, which contains the hydrate.

Consider, for instance, a uniform distribution of hydrates in a porous medium which is initially at a uniform temperature, T_i, and occupies the semi-infinite region, $0 < x < \infty$. Initially, the hydrates are assumed to fill the entire pore volume. At time $t = 0$, the temperature at the boundary, $x = 0$, is raised to a new temperature, T_0, which is higher than T_i, and is held constant thereafter. Hydrate dissociation commences and, as a result, there is a moving interface at some distance, $x = \mathrm{X}(t)$, which separates the water/gas region from the undissociated hydrate region. Thus at any time $t > 0$, the water/gas phase (dissociated hydrate zone) occupies the region, $0 < x < \mathrm{X}(t)$, while the undissociated hydrate zone occupies the region, $\mathrm{X}(t) < x < \infty$; these regions are designated as I and II, respectively.

The water resulting from the dissociation process is assumed to remain motionless and is retained within the pores of the dissociated zone. This assumption restricts the analysis to hydrate saturation values of about 0.3. For the sake of simplicity, we shall assume that the thermophysical properties of each phase are constant. We also neglect viscous dissipation, inertial effects, and rule out the possibility of mutual or external energy transmission. With these restrictions, the differential mass, momentum, and energy balances describing the dissociation process may be written as:

$$\epsilon \frac{\partial \rho_g}{\partial t} + \frac{\partial (\rho_g v_x)}{\partial x} = 0 \quad 0 < x < \mathrm{X}(t), \quad t > 0 \tag{1}$$

$$v_x = -\frac{\kappa}{\mu} \frac{\partial P}{\partial x} \quad 0 < x < \mathrm{X}(t), \quad t > 0 \tag{2}$$

$$\rho_1 C_{p_1} \frac{\partial T_{\mathrm{I}}}{\partial t} + \frac{\partial}{\partial x} (\rho_g C_{p_g} v_x T_{\mathrm{I}}) = k_{\mathrm{I}} \frac{\partial^2 T_{\mathrm{I}}}{\partial x^2} + T\beta \frac{DP}{Dt} \quad 0 < x < \mathrm{X}(t), \quad t > 0 \tag{3}$$

$$\frac{\partial T_{\mathrm{II}}}{\partial t} = \alpha_{\mathrm{II}} \frac{\partial^2 T_{\mathrm{II}}}{\partial x^2} \quad \mathrm{X}(t) < xt > 0 \tag{4}$$

$$\rho_g = \frac{MP}{RT_I} \quad 0 < x < X(t), \quad t > 0 \tag{5}$$

Equations 1 and 2 are the continuity equation and the equation of momentum (Darcy's Law) of the gas in the dissociated phase. Equations 3 and 4 are the energy balances for the dissociated and undissociated phases, respectively. Equation 5 is the equation of state of the gas, assuming ideal behavior.

The boundary and initial conditions associated with the above equations are:

$$T_I = T_0 \quad x = 0, \quad t > 0 \tag{6}$$

$$P = P_0 \quad x = 0, \quad t > 0 \tag{7}$$

$$T_I = T_{II} = T_D \quad x = X(t), \quad t > 0 \tag{8}$$

$$\omega \epsilon \rho_H \frac{dX}{dt} + \rho_g v_x = 0 \quad x = X(t), \quad t > 0 \tag{9}$$

$$k_{II} \frac{\partial T_{II}}{\partial x} - k_I \frac{\partial T_I}{\partial x} = \epsilon \rho_H \Delta H_D \frac{dX}{dt} \quad x = X(t), \quad t > 0 \tag{10}$$

$$P_D = \exp(A - B/T_D) \quad x = X(t), \quad t > 0 \tag{11}$$

$$T_{II} = T_i \quad x = \infty, \quad t > 0 \tag{12}$$

$$T_{II} = T_i \quad 0 < x < \infty, \quad t = 0 \tag{13}$$

$$X(t) = 0 \quad t = 0 \tag{14}$$

Equations 9 and 10 describe the mass and energy balances at the dissociation front, respectively. Equation 11 is a thermodynamic equilibrium relationship (Antoine equation) between the hydrate dissociation temperature, T_D, and the gas pressure, P_D, at the dissociation interface. The quantity ω, in the moving boundary mass balance (Eq. 9), represents the mass of the hydrocarbon gas contained in a unit mass of hydrate, derived from assuming 93.5% occupancy of the cages, using the van der Waals and Platteeuw model (1959); this number, ω, is found to be 0.1265 kg CH_4 per kg hydrate. For lower methane occupancy as well as for other gases or gas mixtures, ω can be easily found.

It is apparent from the preceeding mathematical description that the unknown functions are: $\rho_g(x, t)$, $v_x(x, t)$, $P(x, t)$, $T_I(x, t)$, $T_{II}(x, t)$, and $X(t)$. Under the assumption of negligible work of compression, a similarity solution to the above system of equations may be found as:

$$\frac{T_I - T_0}{T_D - T_0} = \frac{\text{erf}(a\eta + b) - \text{erf}\, b}{\text{erf}(a\xi + b) - \text{erf}\, b} \tag{15}$$

$$\frac{T_{II} - T_i}{T_D - T_i} = \frac{\text{erfc}\, \eta}{\text{erfc}\, \xi} \tag{16}$$

$$P^2 = P_0^2 + 4 \frac{\omega \epsilon \rho_H \alpha_{II} \mu R}{\kappa M} \xi \int_0^\eta T_I(\eta)\, d\eta \tag{17}$$

$$X(t) = \xi \sqrt{4\alpha_{II} t} \tag{18}$$

where the similarity variable, $\eta = x/\sqrt{(4\alpha_{II} t)}$, and the constant, ξ, is the root of the following transcendental equation:

$$a \frac{k_I (T_0 - T_D)}{k_{II}(T_D - T_i)} \frac{\exp[-(a\xi + b)^2]}{\text{erf}(a\xi + b) - \text{erf}\, b} - \frac{\exp(-\xi^2)}{\text{erfc}\, \xi} = \sqrt{\pi}\, \epsilon \frac{\rho_H}{\rho_{II}} \text{St}\, \xi \tag{19}$$

and the parameters, a, b, and St, are given by:

$$a = \left(\frac{\alpha_{II}}{\alpha_I}\right)^{1/2} \tag{20}$$

$$b = C_{p_g} \frac{\omega \epsilon \rho_H \alpha_{II}}{a k_I} \xi \tag{21}$$

$$St = \frac{\Delta H_D}{C_{p_{II}}(T_D - T_i)} \tag{22}$$

Equation 19 involves only physical parameters, boundary and initial conditions, and the constant ξ. This implies that the dissociation temperature, T_D, and the corresponding dissociation pressure, P_D, are independent of time. Furthermore, Eqs. 15 to 19 may be shown by direct substitution, to satisfy the differential equations and the boundary conditions of the problem, Eqs. 1 to 14.

Table 1 shows the values of the physical, thermal, and geological parameters used in the present study. These were obtained from several sources, which include Lewin and Associates (1984).

From Eq. 18, it can be seen that the motion of the dissociation front is proportional to the constant, ξ, which can be determined from Eq. 19. The higher the value of ξ, the faster the movement of the dissociation front. The constant, ξ, may be interpreted as the dimensionless location of the dissociation front, $X(t)/(4\alpha_{II} t)^{1/2}$, and also as the dimensionless dissociation front velocity, $v_D/(\alpha_{II}/t)^{1/2}$, where v_D is the velocity of the dissociation front.

Table 1. Parameters Used in Dissociation Model

Porosity, ϵ	0.3
Permeability, κ	1.38×10^{-13} m^2
Thermal Diffus. of Dissoc. Zone, α_I	2.89×10^{-6} m^2/s
Thermal Diffus. of Hydrate Zone, α_{II}	6.97×10^{-7} m^2/s
Thermal Conductiv. of Dissoc. Zone, k_I	5.57 W/m · K
Thermal Conductiv. of Hydrate Zone, k_{II}	2.73 W/m · K
Hydrate Density, ρ_H	913 kg/m^3
Hydrate Heat of Dissociation, ΔH_D	
$248 < T < 273$ K: $\Delta H_D = 215.59 \times 10^3 - 394.945\, T$	J/kg
$273 < T < 298$ K: $\Delta H_D = 446.12 \times 10^3 - 132.638\, T$	J/kg
Antoine Equation	
$P_D = \exp(49.3185 - 9459/T_D)$	Pa
Gas Heat Capacity	
$C_{p_g} = 1.23879 \times 10^3 + 3.1303\, T + 7.905 \times 10^{-4}\, T^2 - 6.858 \times 10^{-7}\, T^3$	J/kg · K
Gas Viscosity	
$\mu = [2.4504 \times 10^{-3} + 2.8764 \times 10^{-5}\, T + 3.279 \times 10^{-9}\, T^2 - 3.7838 \times 10^{-12}\, T^3] + [2.0891 \times 10^{-5}\, \rho_g + 2.5127 \times 10^{-7} \rho_g^2 - 5.822 \times 10^{-10} \rho_g^3 + 1.8387 \times 10^{-13} \rho_g^4]$	Pa · s

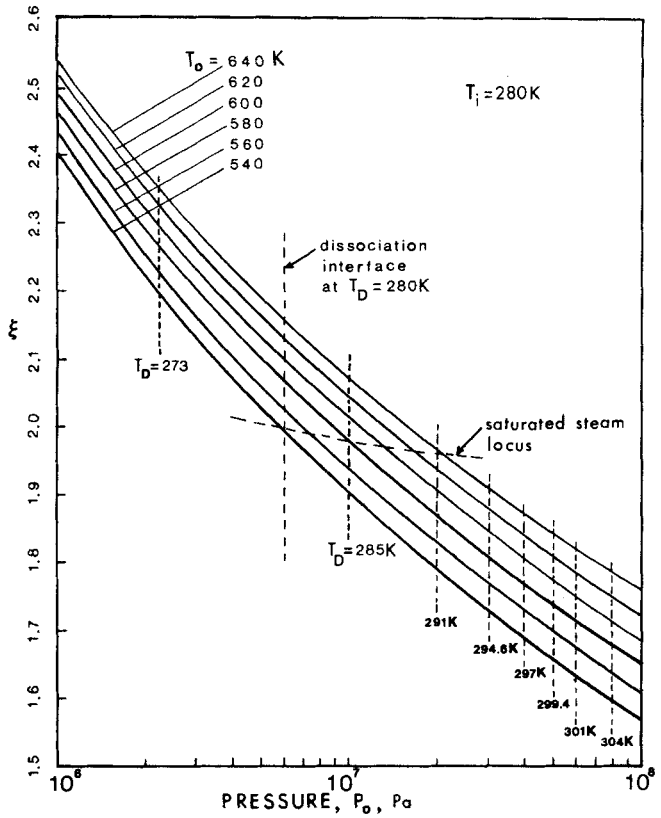

Figure 1. Position of the dissociation front, ξ, vs. T_0 and P_0.

Figure 1 shows typical values of ξ as function of T_0 and P_0, for a hydrate reservoir at an initial temperature, T_i = 280 K. As can be seen, larger values of ξ are obtained when higher temperatures and lower pressures are imposed on the system. Also shown in Figure 1 is the locus of temperatures and pressures, corresponding to saturated steam. Temperature and pressure conditions below this locus correspond to hot water, while those above, correspond to superheated steam. It may be noted that ξ decreases slowly with incresaing pressure along the saturated steam locus. Thus, high pressure saturated steam does not promote hydrate dissociation.

In addition, Figure 1 provides the locus of temperatures and pressures for which the dissociation interface is at the initial temperature of 280 K. For temperature and pressure conditions to the right of this locus, the dissociation temperature is larger than the initial temperature, as indicated by the other constant (vertical) T_D loci shown in the figure. Furthermore, these loci show that higher pressures result in larger values for T_D, while the latter remains essentially independent of T_0.

For conditions of temperatures and pressures to the left of the 280 K locus, the dissociation temperature becomes progressively lower than the initial temperature and may eventually reach the freezing temperature of water, as indicated by the 273 K locus. The latter locus imposes a limitation on the dissociation process; hydrate at the interface dissociates into gas and ice, rather than gas and water. This is an undesirable situation since ice is impermeable and formation of such a layer would stop further hydrate dissociation. Note that this situation arises only under low pressure conditions, in which case, part of the energy of dissociation may be derived from the hydrate reservoir itself.

In order to evaluate the potential of gas production from hydrate reserves using thermal stimulation, calculations were made to determine the energy needed for dissociation, and the amount of gas recovered. To this end, an overall energy efficiency ratio (*E.E.R.*) may be defined as follows:

$$E.E.R. \equiv \frac{G(t) \cdot (H.V.)}{\dot{Q}(t)} \tag{23}$$

where $G(t)$ is the total gas produced up to time t in m^3 CH_4 at STP per unit area of heating surface, $H.V.$ is the heating value of the gas (3.764×10^7 J/m^3 CH_4 at *STP*), and $\dot{Q}(t)$ is the total heat input to the system, up to time t. The quantities, $G(t)$, and $\dot{Q}(t)$, are easily found as:

$$G(t) = 0.17664\, \epsilon \rho_H X(t) \tag{24}$$

$$\dot{Q}(t) = \int_0^t q(0, t)\, dt \tag{25}$$

Using results from the previous solution, it can be shown that the *E.E.R.* is independent of time, and is dependent only on the parameters of the system and the boundary and initial conditions. Using the parameters in Table 1 with an initial temperature of 280 K, the *E.E.R.* was calculated for a wide range of T_0 and P_0. The results are shown in Figure 2. As can be seen, the *E.E.R.* ranges between 6.2 and 11.4, with a value of about 9 for practical values of P_0 and T_0. A value of 9 appears to be encouraging, in view of the fact that it was obtained for a porosity of 0.3. Higher porosities should yield higher values for the *E.E.R.*

Acknowledgment

This work was made possible by support of the United States Department of Energy, through Grant DE-FG21-86MC23063-4. The authors

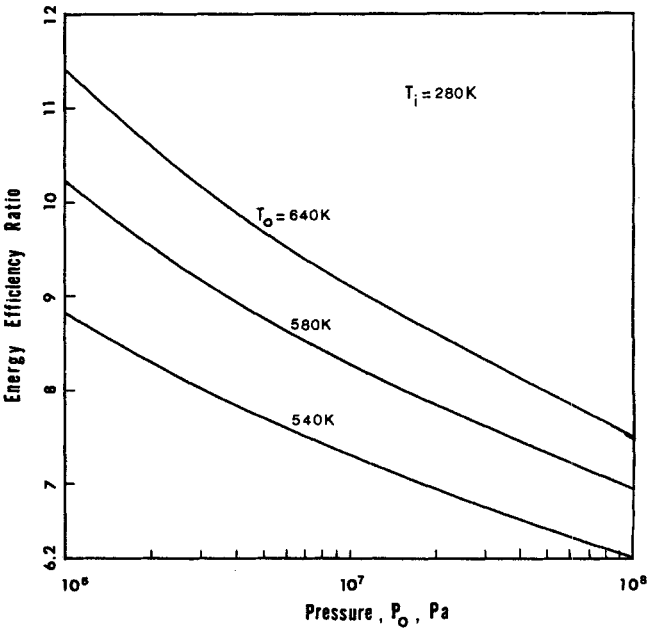

Figure 2. Energy efficiency ratio vs. T_0 and P_0.

wish to express their thanks to Mr. Ali Elkamel for his assistance with the numerical computations.

Notation

C_p = effective heat capacity, J/kg · K
C_{p_g} = gas heat capacity, J/kg · K
$G(t)$ = cumulative gas produced, m^3 gas at STP/m^2
$H.V.$ = heating value of gas, J/m^3 gas at STP
k = effective thermal conductivity, J/s · m · K
M = gas molecular mass, kg/kg-mol
P = gas pressure, Pa
P_0 = pressure at $x = 0$, Pa
P_D = dissociation pressure, Pa
$\dot{Q}(t)$ = cumulative heat input, J/m^2
$q(x, t)$ = heat flux, J/s · m^2
R = universal gas constant, J/kg-mol · K
St = Stefan number, Eq. 22
STP = standard temperature (273.15K), pressure (101,328 Pa)
$T(x, t)$ = temperature, K
T_0 = temperature at $x = 0$, K
T_D = dissociation temperature, K
T_i = initial temperature, K
t = time, s
v_x = superficial gas velocity, m/s
x = axial position, m

Greek letters

α = effective thermal diffusivity, m^2/s
β = coefficient of thermal expansion of gas, K^{-1}
ΔH_D = hydrate heat of dissociation, J/kg
ϵ = porosity
η = similarity variable ($= x/(4\alpha_{II}t)^{1/2}$)
κ = permeability, m^2
μ = gas viscosity, Pa · s
ξ = constant
ρ = effective density, kg/m^3
ρ_g = gas density, kg/m^3
ρ_H = hydrate density, kg/m^3
ω = mass of gas produced per unit mass of hydrate

Subscripts

I = dissociated zone, I
II = hydrate zone, II
D = dissociation
g = gas
H = hydrate
i = initial condition
0 = boundary condition at $x = 0$

Literature Cited

Holder, G. D., P. F. Angert, and S. P. Godbole, "Simulation of Gas Production from a Reservoir Containing Both Gas Hydrates and Free Natural Gas," SPE Meeting, New Orleans, Paper 11005 (1982).

Kamath, V. A., G. D. Holder, and P. F. Angert, "Three Phase Interfacial Heat Transfer During Dissociation of Propane Hydrates," *Chem. Eng. Sci.*, **39**(10), 1435 (1984).

Lewin and Associates, Inc., *Handbook of Gas Hydrate Properties and Occurrence*, DOE/MC/19239-1546, U.S. Printing Office, Washington, DC (1984).

McGuire, P. L., "Methane Hydrate Gas Production by Thermal Stimulation," *Can. Permafrost Conf. Proc.*, R. J. E. Brown Memorial Vol., Calgary, Canada (Mar., 1981).

Selim, M. S., and E. D. Sloan, "Modeling of the Dissociation of an *In-Situ* Hydrate," SPE Calif. Reg. Meet., Bakersfield, Paper 13597 (1985).

Ullerich, J. W., M. S. Selim, and E. D. Sloan, "Theory and Measurement of Hydrate Dissociation," *AIChE J.*, **33**, 747 (1987).

van der Waals, J. H., and J. C. Platteeuw, "Clathrate Hydrates," *Adv. Chem. Phys.*, I. Prigogine, ed. **2**, 1 (1959).

Manuscript received July 29, 1987, and revision received Jan. 25, 1989.

Errata

In the paper entitled, "A Nonrandom Factor Model for the Excess Gibbs Energy of Electrolyte Solutions" by A. Haghtalab and J. H. Vera (**34**, May, 1988, p. 803), Eqs. A7 and A8 of the Appendix should read:

$$(\ln \gamma_{I\pm})_{D-H} = \frac{-A|Z_{Ai}Z_{Ci}|I^{1/2}}{1 + BI^{1/2}} \qquad \text{(A7)}$$

$$(\ln \gamma_W)_{D-H} = \frac{2AM_W}{(10B)^3}\left[1 + BI^{1/2} - \frac{1}{1 + BI^{1/2}} - 2\ln(1 + BI^{1/2})\right] + \ln\left(1 + \frac{\nu M_W m}{1{,}000}\right) - \frac{\nu M_W m}{1{,}000} \qquad \text{(A8)}$$

All results were calculated with the correct equations.